Dynamics of Charged Particles in a Paul Radio-Frequency Quadrupole Trap

J. D. Prestage, A. Williams, L. Maleki, M. J. Djomehri, and E. Harabetian

Jet Propulsion Laboratory, California Institute of Technology, 4800 Oak Grove Drive, Pasadena, California 91109

(Received 1 October 1990)

We have carried out a molecular-dynamics simulation of hundreds of ions confined in a Paul trap. The simulation includes the trapped particles' micromotion and interparticle Coulomb interactions. We have implemented a random walk in velocity to bring the secular motion to a given temperature which we have numerically measured. When the coupling Γ is large the ions form concentric shells which undergo a quadrupole oscillation at the rf frequency, while the ions within a shell form a 2D hexagonal lattice. Ion clouds at 5 mK show no rf heating for $q_z \lesssim 0.6$, whereas rapid heating is seen for $q_z = 0.8$.

PACS numbers: 32.80.Pj, 36.40.+d, 52.25.−b, 52.55.Mg

Several recent experimental and theoretical investigations have studied the dynamics of trapped ions in Paul traps. These studies were motivated by the observation of crystal structures in laser-cooled trapped ions[1] and the observation of chaos in the dynamics of laser-cooled ions.[2] Related theoretical work investigated the formation of crystal structures of highly stripped ions in storage beams.[3] Despite these studies significant questions remain unanswered regarding the structure and dynamics of large ion clouds in Paul traps. Indeed, only one investigation simulating clouds of more than 100 ions has included ion micromotion.[4]

In this Letter we report the results of a molecular-dynamics simulation of many ions in an rf trap which includes the micromotion induced by the rf trapping field, thereby modeling the effect of any rf heating on the structure of the crystallized ion cloud. We have characterized the cloud by its secular temperature, have carried out the first measurements of structure within a crystalline shell at two different temperatures, and have found solid and liquid behavior. Use of the secular temperature allows computation of a coupling parameter Γ which is based upon the random thermal energy of the secular motion and removes the large nonrandom micromotion contribution to a "temperature" assignment of large clouds. In addition, we have for the first time measured rf heating in large clouds at high values of the trapping parameter q. This important feature is unique to Paul traps and, as yet, there is no way to predict the onset and character of this heating since all such previous simulations have dealt with small numbers of ions.

Since the work of Wuerker, Shelton, and Langmuir[5] there has been much progress in storing and cooling both atomic and subatomic particles. The development of laser cooling[6] to temperatures below 10 mK for several thousand ions confined in a Penning trap[7] has led to an interest in crystallization phenomena in these cold multiparticle systems. Indeed, several groups have reported measurements of ordering for small numbers of ions in an rf trap[1,2] while shell structure of 15000 or more ions in a Penning trap has been measured.[8] Motivated by the attainment of such large values of Γ, careful simulations[9] of more than 100 ions in a Penning trap showed shell structure, but some discrepancies with the measured structure were present.

With regard to large ion clouds in Paul traps, it is generally believed that rf heating presents one barrier to laser cooling. That is, ions gain energy from the rf trapping field via interparticle interactions. This effect has been studied in some detail[10,11] and rf heating is found to be quite pronounced near the limits of stable trapping for few-ion systems. Furthermore, the nonlinearity of the equations of motion leads to chaotic behavior in the ionic trajectories.[10,11]

Another barrier to laser cooling is encountered when the ions reside far enough from the central node of the trap so that the amplitude of their micromotion exceeds the wavelength of the cooling radiation.[12] The micromotion broadens the optical linewidth for the majority of ions in a large cloud and can lead to laser heating, thereby preventing crystallization.[12] One solution to this difficulty may be to use the rf trap geometry of Ref. 13 where the rf fields are transverse to the trap longitudinal axis where the cooling laser could be applied.

The equations of motion for several particles held in an rf trap with conventional hyperbolic electrodes are

$$\frac{d^2u_i}{d\tau^2}+[a_r+2q_r\cos(2\tau)]u_i=\frac{4e^2}{m\Omega^2}\sum_j\frac{u_i-u_j}{r_{ij}^3}-\frac{2\mathcal{D}}{\Omega}\frac{du_i}{d\tau}$$

for the x_i and y_i coordinates, and

$$\frac{d^2z_i}{d\tau^2}-[a_z+2q_z\cos(2\tau)]z_i=\frac{4e^2}{m\Omega^2}\sum_j\frac{z_i-z_j}{r_{ij}^3}-\frac{2\mathcal{D}}{\Omega}\frac{dz_i}{d\tau}$$

for the z_i coordinate. In the above, (x_i,y_i,z_i) is the position of the ith charge, $\tau=\Omega t/2$ is the normalized time parameter, where Ω is the angular frequency of the rf trapping field, and r_{ij} is the separation of the ith and jth charge. The confinement forces of the rf trap are described by the terms linear in position coordinate, where

$$a_z=8eV_{\rm dc}/m\Omega^2r_0^2,\quad q_z=4eV_{\rm ac}/m\Omega^2r_0^2,$$

with $a_r=a_z/2$ and $q_r=q_z/2$. e/m is the charge-to-mass ratio of the trapped particles while $V_{\rm dc}$ and $V_{\rm ac}$ are the dc and rf voltages applied to the trap electrodes, respectively. To reach the low temperatures which are of interest for this study, a damping term, proportional to the velocity of each particle, is added to each equation.

These equations of motion are integrated by the fourth-order Runge-Kutta scheme with fixed time step h, which is taken to be $\frac{1}{20}$ of the period of the micromotion frequency Ω. Since we obtained the same results with smaller values of h for all cases reported here, we are confident that h is sufficiently small. The position and velocity of each particle is generated at each integration step and completely determines the state of the ensemble of ions.

As a test of our method we have simulated the conditions of Ref. 5 for 32 trapped dust particles and found the structure shown in Fig. 1. The particles are traced through one cycle of the micromotion showing that secular motion has essentially stopped. The agreement with the measured dust configuration is good considering the variations in e/m among the experimentally trapped dust particles. The crystal of Fig. 1 is the structure obtained in the limit of zero secular temperature or, alternatively, infinite coupling parameter $\Gamma = e^2/ak_BT$, where a is the average nearest-neighbor spacing and T is the temperature of the charges. The dust crystal of Fig. 1 at room temperature has $\Gamma \approx 10^7$ which is orders of magnitude larger than $\Gamma \approx 200$ where the transition to crystal behavior is expected,[14] thus justifying our infinite-Γ or zero-temperature simulation.

To extend our model to trapped ions with nonzero temperature we introduce a random-walk step (RWS) in velocity at each of the fixed time steps of the numerical integration. With this modification the mean square of the velocity will grow linearly with time until the damping term balances the growth at some steady-state energy which depends on the size of the velocity step, δv. Since the rate of growth of mean v^2 due to the random walk is $(\delta v)^2/h$ while the damping of v^2 is at a rate $-2\mathcal{D}v^2$, a steady state of kinetic energy, $m(\delta v)^2/4\mathcal{D}h$, is reached. By use of equipartition of energy we determine that $\delta v = (2\mathcal{D}hk_BT/m)^{1/2}$ will result in steady-state temperature T. The sign of this step is determined by a random-number generator independently for each of the three equations of motion for each time step. We wish to emphasize that this process is a purely computational method of preparing the ion ensemble at a given temperature. Indeed, the RWS and damping of velocity are switched off after a steady-state temperature is reached and all results shown below are obtained as the cloud evolves, influenced only by rf trapping forces and interparticle Coulomb interactions.

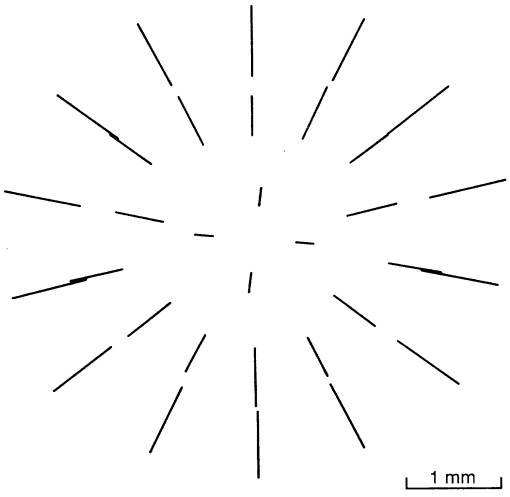

FIG. 1. Simulated crystal structure for 32 Al dust particles suspended in the rf trap of Ref. 5.

The kinetic energy in the secular motion is numerically "measured" over a time interval T_{av} (hundreds of time steps) by measuring the movement of the center position of a particle's rf micromotion. Since the integration time step h is fixed at $\frac{1}{20}$ of the micromotion period, an average of twenty consecutive positions is used to determine the micromotion center. For each Cartesian coordinate, this average position $\bar{x}_i$ is generated for each time step i (the average being computed from the previous twenty time steps) and from that an average velocity is generated, $(\bar{x}_{i+1} - \bar{x}_i)/h = \bar{v}_i$. This is one component of the velocity of the secular motion. From the three velocity components the secular-motion kinetic energy is generated for each time step, averaged over hundreds of time steps and converted to temperature.

Figure 2 shows spherical ($q_z^2/4 = a_z$) ion-cloud configurations at 5 mK for 128, 256, and 512 ions. Particle distance from the $z=0$ plane is plotted against radial distance from the z axis. The position shown is an average over one cycle of the micromotion. During each cycle of the micromotion the shells oscillate between prolate and oblate spheroidal shapes in response to spatial and temporal variation of the trapping fields. The ions were started from rest equally spaced along the four lines $|x| = |y| = |z|$ while the damping time ($=1/\mathcal{D}$) is typically set to five periods of the single-particle secular motion to prepare the ions at temperature T, although a damping time of fifty secular periods also led to crystallization of both the 128-ion and 256-ion cloud. The damping rate $\mathcal{D}$ and the RWS δv were then set to zero. The choice of the higher damping rate corresponds to about 1 mW of UV light on a rapidly cycling transition (e.g., 194 nm Hg^+) and is made largely for the sake of expediency since hours of CPU time can readily be taken during the evolution from initial condition to crystal state. This large damping is essential only for crystallization of large ion clouds with $q_z = 0.8$.

Shell structure is present just as the simulations[9] have shown for ions in a Penning trap, even though the rf trapping mechanism is quite different from the static forces of the Penning trap. In fact, the 256-ion cloud shown in Fig. 3 has shells which contain 6, 30, 77, and 143 ions, which is identical to the results for the 256-ion simulation in the Penning trap.[9] Partial shell structure for 500 ions in an rf trap with $a_z = 0$ was reported in Ref. 4.

From the measured secular temperature and calculat-

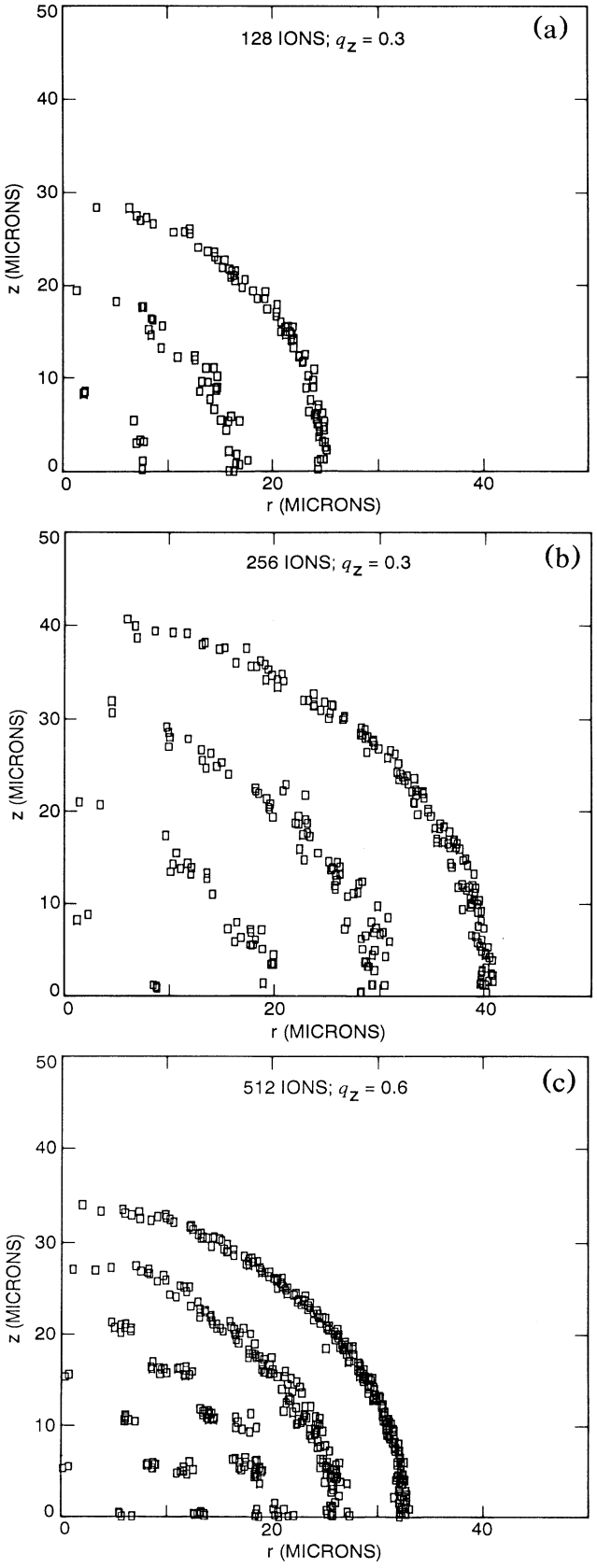

ed Wigner-Seitz radius a the coupling parameter $\Gamma = e^2/ak_BT$ is determined, though, strictly speaking, Γ is time varying for ions confined to a Paul trap. The pseudopotential model is used to determine a using $4\pi a^3 n_0/3 = 1$, where n_0 is the background pseudocharge number density.[11] For $q_z = 0.3$ the radius $a = 7$ μm, and for $q_z = 0.6$, $a = 4.4$ μm.

Ordering within the outer shell of the ion cloud is measured by the coordination-number function $C(s)$ which measures the average number of ions within a distance s of each ion. The correlation function $c(s)$ is given by $\int_0^s 2\pi s c(s) ds = C(s)$. Figure 3 shows these functions plotted for $\Gamma = 477$ ($T_{\text{secular}} = 5$ mK) and for $\Gamma = 60$ ($T_{\text{secular}} = 40$ mK) for the 128-ion cloud. The plot for $C(s)$ at 5 mK shows steps at six and eighteen, indicating that an ion in the outer shell has on average six nearest neighbors and twelve second nearest neighbors. This is characteristic of a 2D hexagonal lattice. The correlation function shows oscillations over the entire measured range of s, indicating long-range order characteristic of a solid. In contrast, the 40-mK ion cloud shows little ordering beyond the range of next-nearest neighbor, which is more characteristic of liquid behavior. This is completely analogous to the simulated behavior of cold ions in a Penning trap.[9]

One way that ion confinement in a Paul trap is very different from confinement in a Penning trap is that ions can gain energy from the rf electric field. Figure 4 shows measured temperatures versus time for several hundred secular periods. The 128-ion cloud at $q_z = 0.3$ shows no heating for the two temperatures which were investigated—5 and 40 mK. Similarly, 256 ions at $q_z = 0.3$ and 512 ions at $q_z = 0.6$ showed 5-mK constant temperature for the 100 secular periods they were simulated. In contrast, at $q_z = 0.8$ there is a clear heating for both the 64- and 128-ion clouds. This rf heating is the large-ion-cloud analog to the crystal melting discussed in Refs. 10 and 11. In the heating state shell structure is still present for the 128-ion cloud as the temperature rises through 100 mK, although continued heating will presumably lead to melting. In addition, the onset of the rf heating for a given q_z is found to depend on the temperature of the cloud. For example, at $q_z = 0.6$ the 128-ion cloud begins rf heating at 100–150 mK. The details of this heating are under study and will be the subject of a future paper.

In summary, we have found stable large cold ion-cloud configurations for ions confined to an rf trap which have shown liquid to solid behavior with no rf heating. For

FIG. 2. Ion-cloud density distributions at 5 mK for (a) 128, (b) 256, and (c) 512 ions held in an rf Paul trap. The 128- and 256-ion configurations are at $q_z = 0.3$ and the 512-ion configuration is at $q_z = 0.6$. Each ion position shown is a time average over one cycle of the rf micromotion. The dc trapping parameter a_z has been adjusted to create a spherical well.

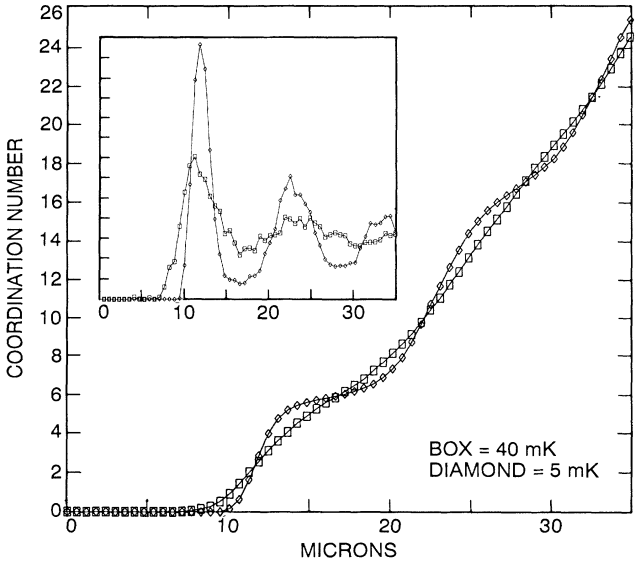

FIG. 3. Coordination-number function in the outer shell of the 128-ion cloud at 5 mK (diamonds) and 40 mK (squares). Each particle has on average six nearest neighbors and twelve second nearest neighbors indicating a hexagonal lattice. Inset: Correlation function showing long-range order of a solid at 5 mK and short-range order of a liquid at 40 mK.

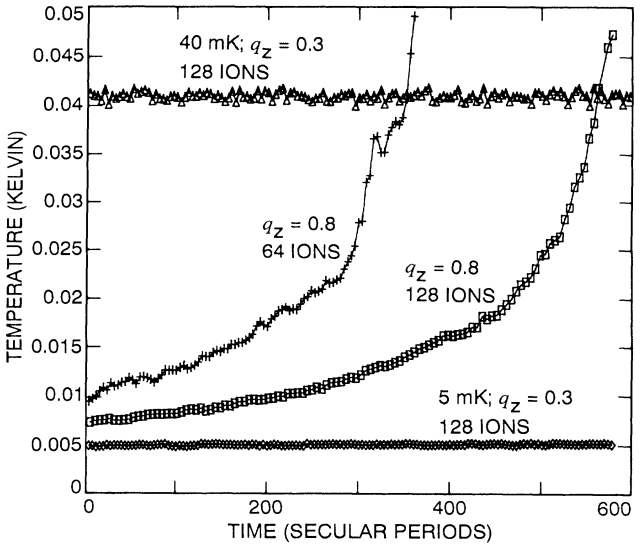

FIG. 4. Temperature evolution for 64- and 128-ion clouds at $q_z = 0.3$ and $q_z = 0.8$. The two heating curves are for 64 ions (left) and 128 ions (right) both at $q_z = 0.8$. The two constant-temperature curves are at $q_z = 0.3$ for 128 ions. Only time-varying trapping fields and interparticle Coulomb interactions are present in this simulated temperature evolution.

the ion clouds investigated here the transition to the rf heating state shows little or no dependence on ion number but depends primarily on q_z and ion temperature. Apparently, there is little or no rf heating for low values of q_z for up to 512 cold ions contained in a Paul trap. Perhaps the only obstacle in obtaining large crystal structures of ions in a Paul trap is that of effectively coupling in the cooling laser power as discussed in Ref. 12. Other issues, however, such as heating caused by simultaneous trapping of ions of different mass, trapping field imperfections, etc., should be investigated.

We wish to acknowledge the use of the Jet Propulsion Laboratory and NASA Ames Numerical Aerodynamic Simulation Cray supercomputers to perform these simulations. We also gratefully acknowledge support from the Caltech President's Fund and NASA Contract No. NAS 7-918.

[1]D. J. Wineland, J. C. Bergquist, W. M. Itano, J. J. Bollinger, and C. H. Manney, Phys. Rev. Lett. **59**, 2935 (1987); Th. Sauter, H. Gilhaus, I. Siemers, R. Blatt, W. Neuhauser, and P. E. Toschek, Z. Phys. D **10**, 153 (1988); R. Casdorff and R. Blatt, Appl. Phys. B **45**, 175 (1988).

[2]F. Diedrich, E. Peik, J. M. Chen, W. Quint, and H. Walther, Phys. Rev. Lett. **59**, 2931 (1987); J. Hoffnagle, R. G. DeVoe, L. Reyna, and R. G. Brewer, Phys. Rev. Lett. **61**, 255 (1988).

[3]A. Rahman and J. P. Schiffer, Phys. Rev. Lett. **57**, 1133 (1986).

[4]R. Blümel, J. Chen, F. Diedrich, E. Peik, W. Quint, and H. Walther, in *Proceedings of the Workshop on Crystalline Ion Beams, Wertheim, Germany* (GSI, Darmstadt, Germany, 1989), p. 194.

[5]R. F. Wuerker, H. Shelton, and R. V. Langmuir, J. Appl. Phys. **30**, 342 (1958).

[6]D. Wineland and H. Dehmelt, Bull. Am. Phys. Soc. **20**, 637 (1975).

[7]L. R. Brewer, J. D. Prestage, J. J. Bollinger, Wayne M. Itano, D. J. Larson, and D. J. Wineland, Phys. Rev. A **38**, 859 (1988).

[8]S. L. Gilbert, J. J. Bollinger, and D. J. Wineland, Phys. Rev. Lett. **60**, 2022 (1988).

[9]D. H. E. Dubin and T. M. O'Neil, Phys. Rev. Lett. **60**, 511 (1988).

[10]J. Hoffnagle, R. G. DeVoe, L. Reyna, and R. G. Brewer, Phys. Rev. Lett. **61**, 255 (1988); R. G. Brewer, J. Hoffnagle, R. G. DeVoe, L. Reyna, and W. Henshaw, Nature (London) **344**, 305 (1990).

[11]R. Blümel, J. M. Chen, E. Peik, W. Quint, W. Schleich, Y. R. Shen, and H. Walther, Nature (London) **334**, 309 (1988); R. Blümel, C. Kappler, W. Quint, and H. Walther, Phys. Rev. A **40**, 808 (1989).

[12]R. G. DeVoe, J. Hoffnagle, and R. G. Brewer, Phys. Rev. A **39**, 4362 (1989).

[13]J. D. Prestage, G. J. Dick, and L. Maleki, J. Appl. Phys. **66**, 1013 (1989).

[14]E. Pollack and J. Hansen, Phys. Rev. A **8**, 3110 (1973); W. L. Slattery, G. D. Doolen, and H. E. DeWitt, *ibid.* **21**, 2087 (1980); **26**, 2255 (1982).